

Advanced Carbon Journal

Advanced Carbon Journal

Adsorptive capture of Cd(II) pollutant from water by a sustainable nanobiosorbent of peanut shell biochar-doped-citric acid

Mohamed E. Mahmoud^{1,*} and Sarah M. Elsayed²

- ¹ Faculty of Sciences, Chemistry Department, Alexandria University, Alexandria, Egypt
- ² Department of Modeling and Simulation, Advanced Technology and New Materials Research Institute (ATNMRI), City of Scientific Research and Technological Applications (SRTA-City), New Borg El-Arab City, 21934 Alexandria, Egypt

Received: 26, 07, 2025; Accepted: 07, 10, 2025; Published: 16, 11, 2025

© 2025 The Author(s). Published by Science Park Publisher. This is an open access article under the CC BY 4.0 license (https://creativecommons.org/licenses/by/4.0/)

Abstract

Cadmium (II) is known as one of the highly toxic metal ions and its release into wastewater effluents must be carefully and efficiently treated prior to discharge into water resources. Therefore, the current investigation is devoted to synthesizing a biochar material from peanut shell waste (PSB) with the aim of further modification with citric acid (CA), as an example of a tricarboxylic organic acid, by microwave irradiation process to generate the desired PSB@CA nanobiosorbent. The produced PSB and PSB@CA were characterized by different techniques confirming the presence of some functional groups related to the O-H, C-H and C=O stretching vibrations. The acquired SEM images of PSB and PSB@CA showed their structures at the nanoscale range providing particle distributions at 22-34 and 19-37 nm, respectively. The as-prepared PSB and PSB@CA nanobiosorbents were compared to identify their incorporated characteristics for Cd(II) ions capture from aquatic systems by the batch technique. The cadmium capacity of PSB@CA was significantly higher than that of PSB, providing strong evidence for the impact of the citric acid modifier. The tricarboxylic groups in CA strongly enhanced the superior binding with Cd(II) ions via cation-exchange, ionpair interaction and complex formation. The maximum capture capacity values of Cd(II) ions were established at the optimum pH 6.0 providing 0.62 and 1.35 mmol g⁻¹ by PSB and PSB@CA, respectively. The equilibrium time at 30 min was characterized by both PSB and PSB@CA. The temperature effect confirmed an endothermic reaction by PSB and PSB@CA providing the maximum Cd(II) adsorption values as 1.35 and 1.66 mmol g⁻¹ at 50 °C, respectively. The ionic strength factor was confirmed to enhance the determined capacity values of Cd(II) from 0.65 to 1.03 mmol g⁻¹ (PSB) and from 1.39 to 1.82 mmol g⁻¹ (PSB@CA) upon increasing the added NaCl concentration from 10 to 100 mgL⁻¹. Moreover, the removal efficiency values of Cd(II) from the spiked 2.0 mg L⁻¹ concentration in tap water, seawater and wastewater were successfully accomplished and corresponded to 98.0, 96.3 and 94.9 ± 0.5 %, respectively. The potential superior validity of PSB@CA in Cd(II) pollutant capture from aquatic systems and real water matrices with excellent efficiency was also demonstrated.

Keywords: Biochar; Peanut shell waste; Citric acid; Cd(II) capture; Adsorption optimization

1. Introduction

Heavy metals are emitted into the environment either naturally or as a result of human activities via point sources such as industrial activities (metal plating, battery manufacturing, paper industries and mining operations) [1]. These metals exhibit hazardous health effects on the

environment and human beings [2]. Moreover, most of these metals are characterized by non-biodegradability and carcinogenicity [3]. The release of heavy metals into water is one of the most serious environmental problems due to the related public health risks [4]. As a consequence, numerous studies have been conducted on coagulation and flotation, reduction and precipitation, ion exchange and electrolysis [5]. However, the documented disadvantages and limitations of these methods have forced the adsorption technique to emerge as an alternative, efficient, and low-cost approach for heavy metals removal from aquatic systems [6]. Therefore, biosorbent-based nanomaterials are considered promising alternatives for heavy-metal removal. Moreover, agricultural by-products and in some cases modified forms could be applied in heavy metals removal from aquatic wastes [7]. Biochar materials are biosorbents produced from agriculture and animal by-products [8]. These are categorized as carbon rich low-cost substances which are produced by thermal decomposition and pyrolysis of the biomass wastes [9].

Cd(II), as a highly toxic heavy metal is generally released to the aquatic effluents by numerous activities such as fossil fuel combustion, and the manufacturing of batteries, plastics, paints and others and thus poses significant risk of toxicity to human health, including potential damage to bones, kidney and other organs [10]. Therefore, great efforts have recently been focused and devoted to remove Cd(II) pollutant from water and waste effluents by implementation of the adsorption technique via numerous biochar materials and other adsorbents or composites [11]. For example, Typha Latifolia biochar/xanthan gum nanosorbent improved cadmium uptake water. A nanocomposite of Typha Latifolia biochar@xanthan gum and thiosemicarbazide (BCXT) was prepared and applied for enhancing Cd(II) adsorption providing 252.3 mg/g capacity [12]. Novel corn straw biochar adsorbents (MCSB) with Mg(II), sodium sulfamate and nZVI were prepared and investigated to remediate Cd(II) with increasing conversion efficiency from 36.98 to 41.61 % [13]. A biochar material was generated from biochar@zeolite composite with nZVI to produce nZVI-BCZo and enhance its adsorption efficiency for Cd(II) and As(III) from wastewater providing the highest capacity at 28.09 and 186.99 mg/g, respectively [14]. A novel biochar composite was synthesized from the combination of biochar with oxalic acid FeS2 to form

FeS₂@OA-BC demonstrating cadmium removal performance corresponding to 74.7 % efficiency [15]. A sludge biochar was prepared and modified with phosphate by impregnation-pyrolysis (PBC) to apply in batch removal of Cd(II) ions showing that the leading mechanism was mainly based on the precipitation (79.94 %) [16]. A sewage sludge biochar (SSB) was prepared by pyrolysis at 700 °C and used to remove Cd(II) pollutant with 97.54 % via physical interaction based on Langmuir isotherm, spontaneous and exothermic process [17]. Moreover, other biochar composites and sorbents were recently implemented for removal of Cd(II) pollutant from aqueous systems [18-20].

Biochars are examples of generated carbonaceous materials from low-cost biomass feedstocks of different origins including animal and agriculture residues by using different pyrolysis approaches [21]. Biochars are rich in carbon-oxygen functionalities as well as high stability, good porosity and large area which are generally produced in specific oxygenated environments [22]. Therefore pristine biochars were applied as adsorbents in removal of some pollutants, but low removal efficiency have limited their generalization in water treatment contaminants [23]. To solve this problematic issue, surface modification of biochar materials with selected compounds is commonly used to incorporate some specific functional groups for the aimed application purposes [24-28]. Based on the above mentioned facts, the novelty in this investigation is mainly related to the design and assembly of a novel nanobiosorbent from the combination of two low-cost materials, a derived biochar from peanut shell waste (PSB) and citric acid (CA) for the formation of an ecofriendly and renewable PSB@CA by using a facile microwave irradiation process. Citric acid, a tricarboxylic acid derivative was selected as an organic modifier due to its aliphatic nature to improve the surface of PSB@CA with high contents of carboxylic acid groups to enable superior capturing of cationic pollutants. It was also aimed to compare the adsorption performance of PSB and PSB@CA toward Cd(II) removal from aquatic systems by the batch system. The two generated nanobiosorbents, PSB and PSB@CA were characterized and their comparative Cd(II) removal capabilities were tested, monitored and optimized in numerous experimental controlling conditions.

2. Experimental

2.1. Instrumentations and materials

The applied instrumentations are fully described in Table 1S (Supplementary Material). The employed chemicals were of high purity and collected from Aldrich Chemical Company. A $0.01 \text{ mol } L^{-1} \text{ Cd(II)}$ stock solution was prepared and the pH of Cd(II) solutions was adjusted in the range pH 1.0-7.0 by the addition of drops of NaOH or HCl ($0.01 \text{ mol } L^{-1}$).

2.2. Synthesis of pristine biochar (PSB) and modified nanobiosorbent (PSB@CA)

Pristine biochar (PSB) was prepared from peanut shell waste after washing several times with distilled water (DW) to remove any impurities. This was then collected, dried and heated in a muffle furnace at 350 °C for 2 h. The collected material was washed and dried at 70 °C for 6 h to produce PSB. The modified biochar PSB@CA was prepared by mixing PSB (5.0 g) with 10 mL DW and 3.0 g citric acid as the organic modifier. All components were thoroughly ground and heated in a microwave oven until almost dry. The heating process was repeated four times to ensure complete binding of citric acid to the surface of PSB for the generation of modified PSB@CA nanobiosorbent.

2.3. Optimization of Cd(II) pollutant capture performance by PSB and PSB@CA

Batch sorption experiments for Cd(II) removal were conducted in this work. The influence of mass factor was studied using different dosages of PSB and PSB@CA (5.0-100.0 mg). A 10.0 mL of Cd(II) solution (0.01 mol L⁻¹) was added to the selected dose and agitated for 30 min. The adsorbed Cd(II) on the surface of PSB and PSB@CA were filtered, washed with 20.0 mL DW and the unreacted ions were analyzed by EDTA titration using xylenol orange—hexamine mixture. This procedure was repeated 3x and the average Cd(II) sorption capacity was concluded from Equation (1).

$$q = (C_i - C_r) V/M \qquad (1)$$

Where q is the metal sorption capacity (mmol g^{-1}) corresponding to the amount of Cd(II) (mmol) adsorbed per gram of PSB or PSB@CA. C_i is Cd(II) initial mol L^{-1} , C_r is Cd(II) residual mol L^{-1} , V (mL) is the aqueous volume and M is the mass (g) of nanobiosorbent.

The influence of pH factor was conducted by adding 20 mg of PSB or PSB@CA to 10.0 mL of Cd(II) (0.01 mol L⁻¹) and adjusting to pH 1.0-7.0 by HCl or NaOH solution (0.01 mol L⁻¹). These were shaken for 30 min, while the residual Cd(II) was figured out to compute the sorption capacity.

The influence of the time factor was accomplished by reacting $10.0\,\text{mL}$ of $0.01\,\text{mol}$ L⁻¹ Cd(II) with $20\,\text{mg}$ of PSB or PSB@CA at the optimum pH $6.0\,\text{condition}$ and selected duration (1-30 min), while the residual Cd(II) ions were determined to compute Cd(II) sorption capacity.

The initial Cd(II) concentration factor was investigated by adding 10 mL of $0.002-0.020 \text{ mol L}^{-1} \text{ Cd(II)}$ solutions to 20 mg of PSB or PSB@CA at the optimum pH 6.0 condition and 30 min, while the residual Cd(II) ions were figured out to compute Cd(II) sorption capacity.

The sorption capacity values of Cd(II) ions were investigated in the presence of diverse ionic strength conditions by the addition of 10-100 mg NaCl to 0.01 mol L⁻¹ Cd(II) solutions and 20 mg of PSB or PSB@CA. These mixtures were shaken for 30 min and the residual Cd(II) ions were determined to compute Cd(II) sorption capacity.

The temperature factor was investigated by adding 10.0 mL of 0.01 mol L⁻¹ Cd(II) to 20 mg of PSB or PSB@CA at the optimum pH 6.0 condition. The reaction mixture was shaken for 30 min at various temperature values from 25 to 50 °C by a thermostated shaker, while the residual Cd(II) ions was figured out to compute Cd(II) sorption capacity.

Regeneration and reutilization of the modified PSB@CA nanobiosorbent after initial removal reaction of Cd(II) pollutant was also explored to evaluate its economic feasibility. Therefore, the regeneration step of the loaded Cd(II) ions onto PSB@CA was performed by treatment with 0.1 mol L-1 HCl as the recycling agent. The recycled PSB@CA was washed with DW, dried and then used in further removal processes of Cd(II) pollutant from aqueous solution. The recycling and regeneration procedures were repeated four more times to complete five successive regeneration tests.

The application of PSB@CA in potential removal application of Cd(II) from polluted natural seawater, wastewater, and tap water samples was investigated by the batch approach. An amount of 50 mg of PSB@CA was used in this respect to remove the spiked Cd(II) concentrations (2.0 & 5.0 mg/L) from 50 mL of these matrices. These samples were shaken for

30 min and the adsorbed Cd(II) ions on the surface of PSB@CA were filtered and the concentration of unreacted Cd(II) ions in the filtrate was determined by atomic absorption spectroscopy to figure out the percentage removal values (R%).

3. Results and discussion

3.1. Characterization

The FT-IR spectroscopy is an effective technique in the analysis and characterization of incorporated functionalities in biochar nanobiosorbents and other materials [29]. Therefore, the FT-IR spectra of PSB and PSB@CA were acquired and compared as illustrated in Figure 1. The FT-IR spectrum of PSB (Figure 1a) is characterized by a series of peaks denoting the nature of this nanobiosorbent as represented by the broad peak at 3400-3600 cm⁻¹ for the O-H stretching. The band at 2924 cm⁻¹ is attributed to C-H interaction on PSB-surface, while the peak at 1620 cm⁻¹ is assigned to C=O stretching. The 1425 cm⁻¹ band corresponds to methyl group δ (C-H), and the band range at 1200-1280 cm⁻¹ is mainly correlated to the aromatic moiety. Finally, the FT-IR of PSB@CA (Figure 1b)

exhibits most of the above mentioned peaks in PSB, but the intense peak at 1650 cm⁻¹ is attributed to the conjugated C=O stretching in carboxylic groups via surface loading of CA onto PSB [30].

The SEM analysis is one of the most powerful techniques for acquiring surface images of nanobiosorbents [31]. Therefore, the SEM studies and images of PSB and PSB@CA were acquired to evaluate the surface morphology of the two assembled nanobiosorbents as illustrated in Figure 2. The SEM image of PSB (Figure 2a) exhibited smooth distribution of homogeneous semi-spherical particles with some incorporated porosity character providing particle size range at 22-34 nm to enable good binding and capturing of the target Cd(II) pollutant. Figure 2b represents the SEM of PSB@CA and the surface of this nanobiosorbent was also observed in the nanoscale particle size ranging from 19 nm to 37 nm, indicating the direct and successful loading of CA on the surface of PSB biochar. Therefore, the assembled PSB@CA nanobiosorbent is expected to enhance the uptake capability for Cd(II) binding with the surface functional carboxylic groups.

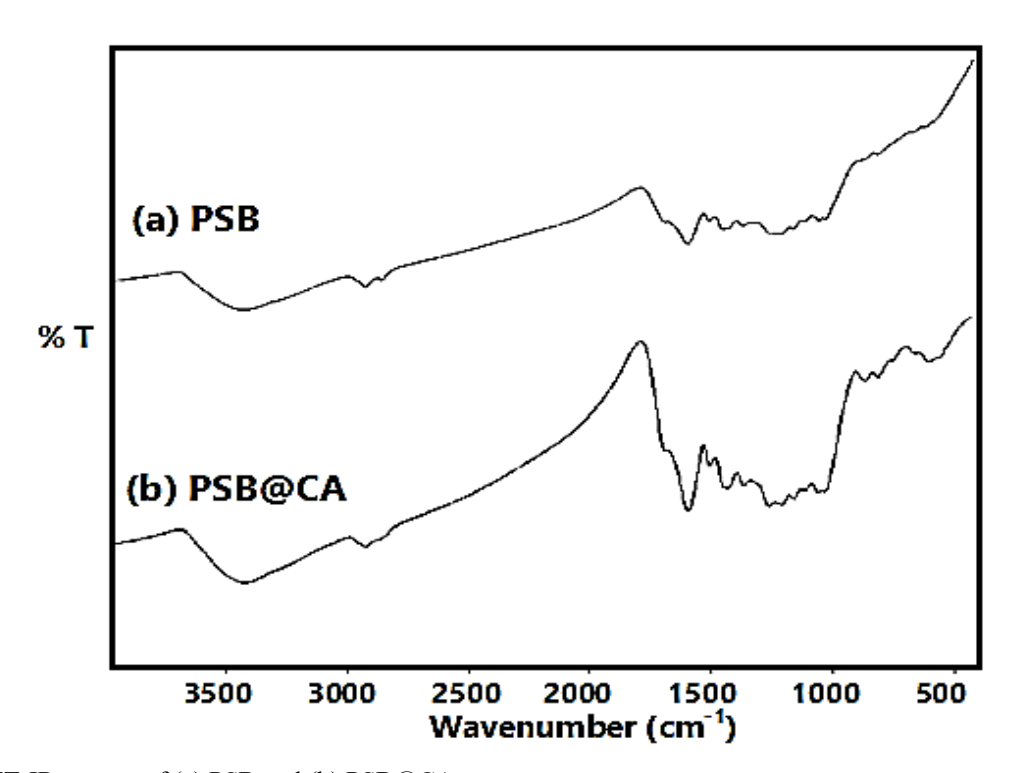


Figure 1. FT-IR spectra of (a) PSB and (b) PSB@CA.

DOI: 10.62184/acj.jacj1000202522

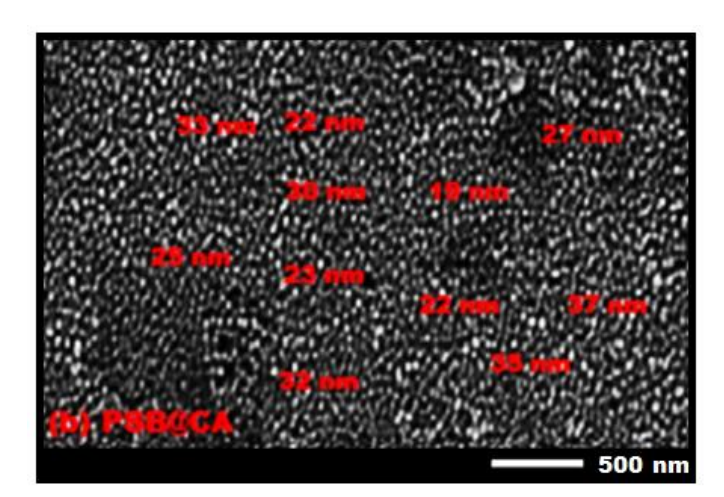


Figure 2. SEM images of (a) PSB and (b) PSB@CA.

Thermal gravimetric analysis (TGA) is commonly employed to determine the thermal stability/degradation of materials under investigation [32]. Figure 3 shows the thermograms of PSB and PSB@CA. Four decomposition steps occurred in the case of PSB (Figure 3a) at 26.5-85.4 °C (mass loss 3.8 %) due to water volatilization from the surface of PSB. The second step at 85.4-284.2 °C (loss 2.9 %) and this corresponds to the partial decomposition of some surface functionalities, while the third step at 284.2-365.3 °C (19.8 %) corresponds to decomposition of the carbonic structure. The fourth step at the range 365.3-562.2 °C with mass loss corresponding to 71.4 % loss. On the other hand, Figure 3(b) represents the TGA thermogram of PSB@CA and also showed four different degradation steps at 24.90-182.7 °C (4.7 % mass loss), 182.7-252.6 °C (19.6 % mass loss), 252.6-365.7 °C (11.4 % mass loss) and 365.7-599.5 °C (39.8 % mass loss). These successive steps are mainly correlated to thermal desorption of adsorbed water molecules, partial and complete thermal decomposition of the surface loaded CA modifier and decomposed carbon skeleton [33]. Finally, the total percentage losses from PSB and PSB@CA nanobiosorbents upon heating to 600 °C were corresponding to 97.9 % and 75.5 % to confirm more incorporated thermal stability characters in PSB@CA by loading citric acid as an organic modifier.

3.2. Comparative sorption behavior of Cd(II) ions onto PSB and PSB@CA nanobiosorbents

Batch equilibrium technique was implemented in this study to compare the adsorptive performance of pristine PSB

and modified PSB@CA nanobiosorbents and examine their applicability in Cd(II) pollutant capture. The effect of different experimental control parameters on the sorption process was examined and optimized under various conditions including pH, contact time, nanobiosorbent dosage, initial Cd(II) concentration, temperature and ionic strength, while the Cd(II) capacity in mmol g⁻¹ was calculated from Equation (1) [34].

3.2.1. Impact of diverse nanobiosorbent dosages on Cd(II) capture by PSB and PSB@CA

The effect of different dosages of PSB and PSB@CA on capacity of Cd(II) ions was carried out and compared by using 5.0-100.0 mg of each nanobiosorbent according to Equation (1). The average values of triplicate results are compiled in Table 1 and expressed in metal capacity value versus nanobiosorbent dosage. It is evident that the related capacity values by PSB@CA nanobiosorbent were significantly higher than those of PSB to provide excellent evidence for the impact of citric acid modifier. The tricarboxylic groups in CA were shown to strongly enhance and improve the direct and superior binding to Cd(II) ions via cation-exchange, ion-pair interaction and complex formation. The maximum Cd(II) ions capacity (mmol g-1) by PSB@CA and PSB were 2.55 and 1.07 mmol g-1, respectively upon using 5.0 mg nanobiosorbent. This can be directly correlated and interpreted by the increased ratio of Cd(II) ions in contact solution versus nanobiosorbent dosage [35]. It was also detected that the capacity values for Cd(II) ions were decreased upon increasing nanobiosorbent mass to 100 mg, providing 0.29 and 0.13

mmol g⁻¹ for PSB@CA and PSB. Such decrease is mainly attributed to the small ratio of metal ions in solution compared to the high nanobiosorbent dose [36].

3.2.2. Impact of diverse pH conditions on Cd(II) capture by PSB and PSB@CA

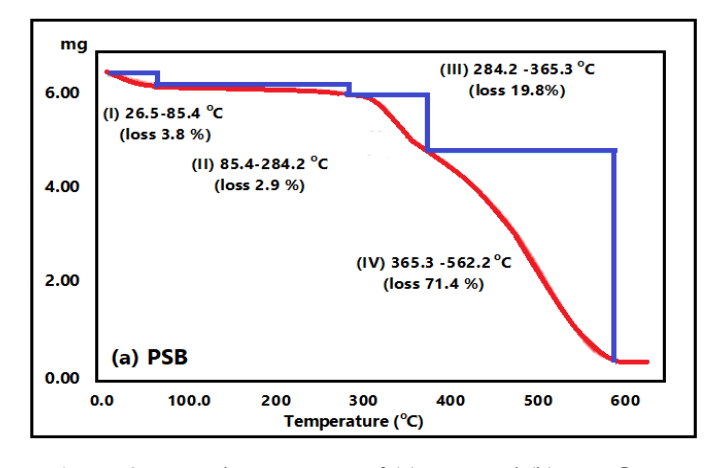
The assistance of pH on Cd(II) pollutant removal performance by pristine PSB and modified PSB@CA is a crucial factor in determining and evaluating the removal efficiency by the assembled nanobiosorbents. The pH of contact solution is known to play a significant role in affecting the protonation degree of surface groups and the investigated Cd(II) pollutant [37]. Therefore, the effect of contact pHs (pH 1.0-7.0) on the Cd(II) capacity was studied (Figure 4). It is evident that the modified PSB@CA nanobiosorbent was confirmed with high incorporated capabilities for Cd(II) pollutant removal from aqueous solution due to the loaded citric acid. The concluded capacity values of Cd(II) (mmol g⁻¹) are referring to low removal efficiency at pH 1 and 2 by the two investigated nanobiosorbents providing 0.26 and 0.35 mmol g⁻¹ (pH 1.0) as well as 0.34 and 0.49 mmol g⁻¹ (pH 2.0)

by PSB and PSB@CA, respectively. This behavior could be assigned to electrostatic repulsion between the protonated surface and Cd(II) cations [38]. However, by enhancing the pH to 6.0, maximum removal values of Cd(II) were established providing 0.62 and 1.35 mmol g⁻¹ (pH 6.0) by PSB and PSB@CA, respectively to refer to the ability of Cd(II) to strongly interact and bind to the surface at almost neutral pH conditions (pH 6.0-7.0).

3.2.3. Impact of diverse reaction times on Cd(II) capture by PSB and PSB@CA

The impact of diverse reaction durations on Cd(II) pollutant removal by the assembled PSB and PSB@CA was accomplished in the same way by the batch technique as an important and critical factor in the removal process. This may be related to the dependence of the adsorption technique on this parameter [39].

Therefore, the shaking time influence on Cd(II) capacity by PSB and PSB@CA nanosorbents was determined by using time range from 2 to 60 min at pH 6.0 as provided in Figure 5.



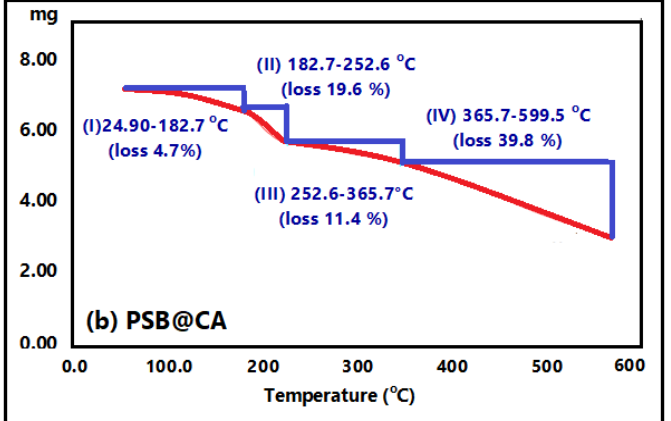


Figure 3. TGA thermograms of (a) PSB and (b) PSB@CA.

Table 1. Effect of nanobiosorbent dosages.

(Conditions: $10 \text{ mL} \text{ of } 0.01 \text{ mol } \text{L}^{-1} \text{ Cd(II)}$, time = 30 min, mass 5-100 mg)

Nanobiosorbent	Metal capacity of Cd(II) in mmol g-1 at diverse nanobiosorbent dosages (mg)*										
	5	10	20	30	40	50	60	70	80	90	100
PSB@CA	2.55	2.37	2.01	1.76	1.52	1.28	0.90	0.73	0.51	0.37	0.29
PSB	1.07	0.98	0.76	0.65	0.46	0.30	0.22	0.18	0.15	0.14	0.13

^{*} Values are the average metal capacity of Cd(II) in mmol g⁻¹ based on triplicate runs with RSD = 1.4- 2.9 %).

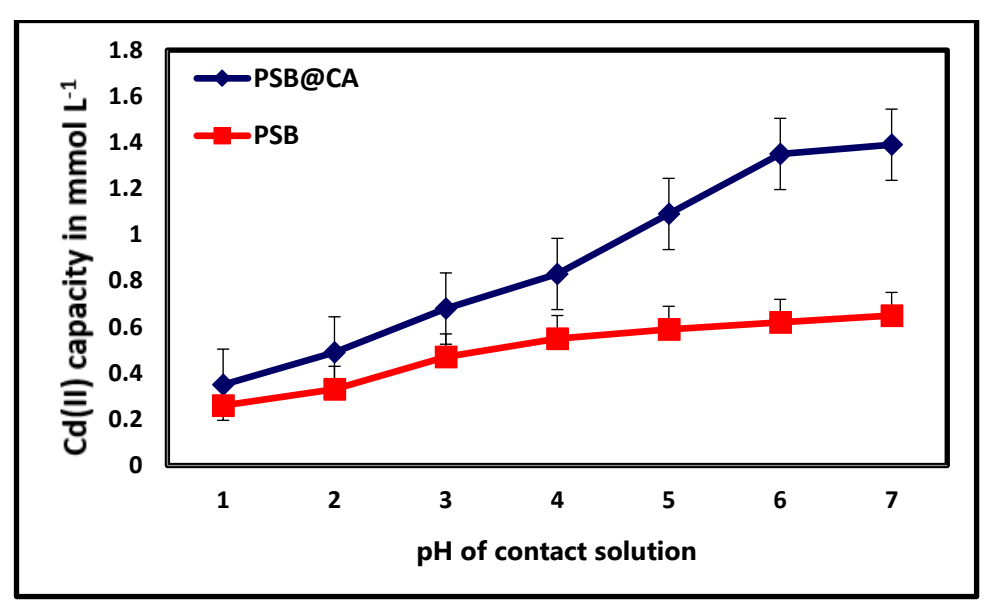


Figure 4. Effect of pH conditions on Cd(II) removal by PSB and PSB@CA.

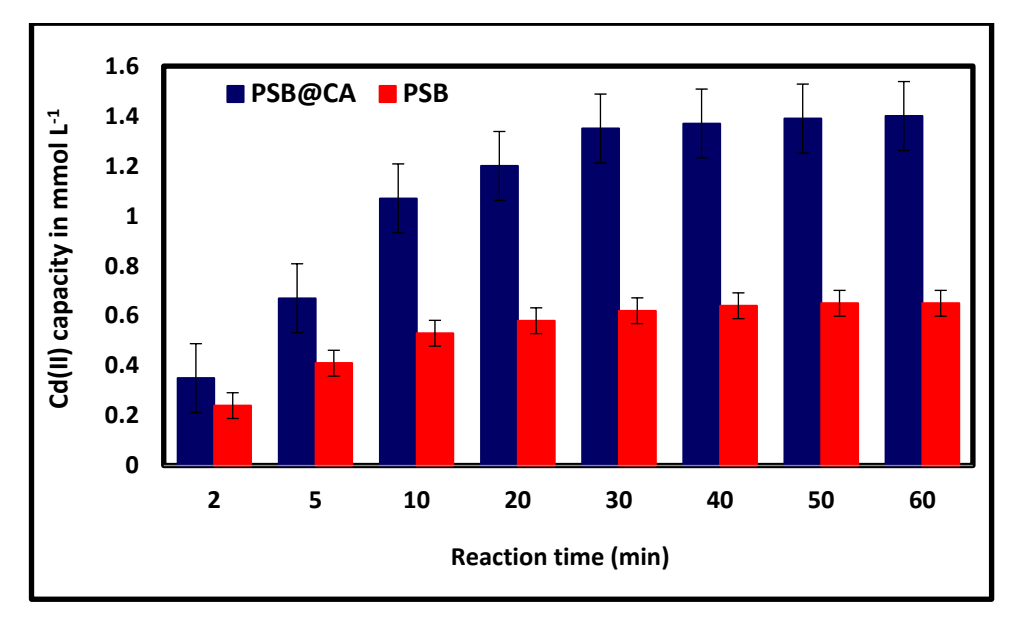


Figure 5. Effect of reaction time conditions on Cd(II) removal by PSB and PSB@CA.

As demonstrated, a gradual increasing orders in the metal capacities of Cd(II) ions by the two investigated nanobiosorbents were increased from 2.0 min up to 30 min to reach to the equilibration time at 30 min. The characterized capacities of Cd(II) ions by PSB and PSB@CA were identified as 0.24 and 0.35 mmol g⁻¹ (2.0 min), 0.53 and 1.07 mmol g⁻¹ (10.0 min), and 0.62 and 1.35 mmol g⁻¹ (30.0 min), respectively. After the equilibration time, slight increase in capacity values of Cd(II) ions by PSB and PSB@CA were reached to 0.65 and 1.40 mmol g⁻¹ (60.0 min). Finally, the

concluded Cd(II) pollutant capacity values refer to the superiority of PSB@CA compared to PSB in terms of the played role by the surface incorporated tricarboxylic acid functionalities in enhancing and improving the direct binding reaction with Cd(II) ions [40].

3.2.4. Impact of diverse Cd(II) concentration on Cd(II) capture by PSB and PSB@CA

The influencing role of Cd(II) ions concentration is another significant impacting factor on the adsorption behavior of the assembled pristine PSB and modified

PSB@CA. Therefore, this assessment study was conducted to compare the removal performance of PSB versus PSB@CA by reacting the selected Cd(II) concentration (0.002 -0.020 mol L⁻¹) with 20 mg of nanobiosorbent at the optimum pH 6.0 condition and 30 min duration. As demonstrated in Table 2. the Cd(II) capacity by both PSB and PSB@CA was found to improve by increasing Cd(II) concentration. For example, the removal efficiencies of Cd(II) ions by PSB were corresponding to 0.16, 0.62 and 1.39 mmol g⁻¹ by using 0.002, 0.010 and 0.020 mol L-1, respectively, while PSB@CA exhibited 0.29, 1.35 and 2.38 mmol g⁻¹ by using 0.002, 0.010 and 0.020 mol L-1, respectively. Such improvement in the capacity value at higher Cd(II) concentration is correlated to high ratio of Cd(II) ions compared to the loaded active sites on the evaluated nanobiosorbent. Additionally, the confirmed capture values of Cd(II) pollutant by PSB@CA were higher when compared to those related to PSB to verify the role of increased number of surface loaded carboxylic groups in enhancing the direct metal ions binding [41].

3.2.5. Impact of diverse temperatures on Cd(II) capture by PSB and PSB@CA

The impacting role of temperature on Cd(II) capture efficiency by the assembled pristine PSB and modified PSB@CA were investigated to asses the temperature contribution on the uptake values and characterize the endothermic or exothermic nature. This study was accomplished by mixing 10 mL of 0.01 mol L⁻¹ Cd(II) with 20.0 mg dosage at pH 6.0 and shaking the reaction mixture for 30 at temperature range from 25-50 °C as compiled (Table 3). The observed trends are mainly denoting to the increase in Cd(II) capacity by raising the temperature from 25 to 50 °C to confirm an endothermic reaction by the two investigated PSB and PSB@CA nanobiosorbents. The characterized capacity values of Cd(II) ions by PSB were enhanced and identified to

increase from 0.62 to 0.91 mmol g⁻¹ by increasing the temperature from 25 to 55 °C, respectively, while the values by PSB@CA nanobiosorbent at the same two temperatures were corresponding to 1.35 and 1.66 mmol g⁻¹, respectively. As indicated, the outcomes of this study are denoting that the binding reactions of Cd(II) pollutant onto PSB and PSB@CA nanobiosorbents are basically dependent on an endothermal reaction. Moreover, the superior uptake behavior of PSB@CA when compared to PSB is mainly attributed to the high binding and chelating efficiency of citric acid by the three incorporated carboxylic groups [42].

3.2.6. Impact of diverse ionic strength conditions on Cd(II) capture by PSB and PSB@CA

As outlined, the surfaces of assembled PSB and PSB@CA nanobiosorbents are mainly composed of negatively charged functional groups as -OH and -COOH. Therefore, these functionalities are expected to highly contribute to the adsorption reaction of the target cationic Cd(II) pollutant by the presence of high ionic strength from Na⁺ ions. Therefore, the ionic strength impact was testified by the addition of NaCl doses (10-100 mg) to the reaction which was composed from the mixing of 10.0 mL of 0.01 mol L⁻¹Cd(II) with 20.0 mg PSB or PSB@CA at pH 6.0 and 30 min reaction time. As listed in Table 4, the capture behaviors of Cd(II) pollutant by the investigated PSB and PSB@CA nanobiosorbents were identified to follow increasing orders of determined capacity values from 0.65 to 1.07 mmol g⁻¹ and from 1.39 to 1.85 mmol g⁻¹, respectively upon increasing the added NaCl from 10 to 100 mg. It is also evident that the increase in Cd(II) uptake by PSB@CA may be correlated to the hydrogen ions exchange by Na⁺ in the carboxylic groups and this contributed to the increasing binding capability of these groups with Cd(II) ions in solution via cation-exchange mechanism [43].

Table 2. Effect of diverse initial concentration conditions of Cd(II).

(Conditions: time = mass 20 mg, Time 30 min, pH 6.0, 10 mL of 0.002-0.020 mol L^{-1} Cd(II))

Nanobiosorbent	Metal capacity of Cd(II) in mmol g-1 at diverse Cd(II) concentrations (mol L-1)*									
	0.002	0.004	0.006	0.008	0.010	0.012	0.014	0.016	0.018	0.020
PSB@CA	0.29	0.52	0.81	0.16	1.35	0.166	0.189	0.203	0.219	2.38
PSB	0.16	0.28	0.39	0.50	0.62	0.85	0.97	1.17	1.28	1.39

^{*} Values are the average metal capacity of Cd(II) in mmol g^{-1} based on triplicate runs with RSD = 1.0-3.3 %).

Table 3. Effect of diverse reaction temperature conditions.

(Conditions: 10 mL of 0.01 mol L⁻¹ Cd(II), time = 30 min, mass = 20 mg, pH = 6.0, temperature range = 25-50 °C)

Nanobiosorbent	Metal capacity of Cd(II) in mmol g-1 at diverse reaction temperature conditions*									
	25 °C	30 °C	35 °C	40 °C	45 °C	50 °C				
PSB@CA	1.35	1.39	1.46	1.50	1.61	1.66				
PSB	0.62	0.68	0.74	0.79	0.86	0.91				

^{*} Values are the average metal capacity of Cd(II) in mmol g^{-1} based on triplicate runs with RSD = 0.8- 2.5 %).

Table 4. Effect of diverse ionic strength conditions.

(Conditions: 10 mL of 0.010, time = 30 min, mass 20 mg, pH 6.0, added NaCl = 10-100 mg)

Nanobiosorbent	Metal capacity of Cd(II) in mmol g-1 at diverse ionic strengths of NaCl (Mg)*									
	10	20	30	40	50	60	70	80	90	100
PSB@CA	1.39	1.44	1.53	1.59	1.65	1.70	1.74	1.77	1.81	1.85
PSB	0.65	0.72	0.77	0.83	0.87	0.92	0.96	1.01	1.04	1.07

^{*} Values are the average metal capacity of Cd(II) in mmol g^{-1} based on triplicate runs with RSD = 1.6-3.7 %).

Finally, the superior capture behavior of PSB@CA compared to PSB is also confirmed by the impact of ionic strength factor as illustrated in Table 4.

3.2.7. Regeneration and reutilization of the modified PSB@CA nanobiosorbent

Regeneration and reutilization of the modified PSB@CA nanobiosorbent after initial removal reaction of Cd(II) pollutants is a significant step in terms of the economic feasibility [44]. Therefore, the regeneration step of the loaded Cd(II) ions onto PSB@CA was performed via treatment with 0.1 mol L-1 HCl as the recycling agent. The recycled PSB@CA was then used in additional removal processes of Cd(II) pollutant. After the first regeneration step, the percentage uptake value of Cd(II) pollutant was corresponded to 1.29 mmol g-1 to confirm 95.56 % stability. Moreover, the regenerated PSB@CA after the fifth recycling procedure was found to efficiently remove Cd(II) ions with 1.17 mmol g-1 to confirm 86.67 % stability and thus additionally refer to the high incorporated stability of PSB@CA nanobiosorbent under the recycling condition.

3.2.8. Water remediation of Cd(II) pollutant by PSB@CA

The potential remediation of Cd(II) pollutant from various samples by the action of modified PSB@CA nanobiosorbent was also investigated as an important practical procedure. The selected water samples (tap water, sea water and wastewater)

were collected and spiked to generate 2.0 and 5.0 mg L-1 concentration of Cd(II). 50 mL of these samples were mixed and reacted with 50 mg of PSB@CA and subjected to batch removal process by shaking for 30 min. The removal (%) of Cd(II) was determined by the atomic absorption analysis and the outcomes of this study were computed to confirm the removal efficiency values from the spiked 2.0 mg L⁻¹ concentration, providing 98.0, 96.3 and 94.9 \pm 0.5 % from tap water sea water and wastewater, respectively. Similarly, the spiked 5.0 mg L⁻¹ concentration in tap, sea, and wastewater were characterized to exhibit high removal percentages providing 96.4, 93.5 and 92.6 \pm 0.7 %. Hence, the investigated and evaluated PSB@CA strongly denotes to the applicability and visibility of this modified nanobiosorbent for the treatment of Cd(II) pollutant from waste effluents, providing excellent Cd(II) capture performance.

4. Conclusion

A facile, rapid and green microwave-assisted procedure was employed to covalently bind peanut shell biochar (PSB) with tricarboxylic citric acid for the formation of the modified PSB@CA nanobiosorbent without any organic or hazardous solvent. PSB@CA was efficiently produced from low cost waste materials and modified with ecofriendly and biodegrable citric acid as a surface modifier to improve the uptake performance towards cationic pollutants as Cd(II) pollutant. The two biosorbents, PSB and PSB@CA, were

explored and compared in Cd(II) pollutant capture from aquatic systems. Superior performance of PSB@CA toward removal and capture of Cd(II) were concluded from all explored and investigated experimental controlling factors when compared to PSB. The tricarboxylic groups in PSB@CA strongly support the superior binding with Cd(II) ions via cation-exchange, ion-pair interaction and complex formation. The ionic strength factor was identified to intensify the assessed Cd(II) capacity from 1.39 to 1.82 mmol g-1 (PSB@CA) with NaCl concentrations rising from 10 to 100 mg. PSB@CA showed high stability and reusability during regeneration cycles and referred to excellent performance after the first regeneration step providing 1.29 mmol g⁻¹ Cd(II) pollutant removal to confirm 95.56 % stability and the fifth recycling procedure afforded efficient Cd(II) ions removal with 1.17 mmol g⁻¹ to refer to 86.67 % stability. Moreover, the removal efficiency values of Cd(II) from tap, sea, and wastewaters were successfully accomplished, providing 98.0, 96.3 and 94.9 \pm 0.5 % from the spiked 2.0 mg L⁻¹ concentration, respectively. Collectively, these findings confirm the promising applicability of PSB@CA as an efficient, sustainable, and renewable nanobiosorbent for the remediation of Cd(II) pollutant from both laboratory-prepared solutions and real aquatic systems.

Nevertheless, two main limitations should be noted. Firstly, the current study was exclusively focused on Cd(II) as the only model pollutant. Secondly, the adsorption experiments were performed using the batch technique, which is inherently limited in treating large sample volumes. To overcome these limitations, future works are suggested to focus on extending the application of PSB@CA to the removal of other hazardous organic and inorganic contaminants from wastewater. For practical large-scale water treatment applications, it is suggested to scale up the process by employing dynamic column techniques.

Author contribution

Mohamed E. Mahmoud: Concept, Supervision and Writing-Editing-Review.

Sarah M. Elsayed: Experimental work, Data collection and Writing-Editing.

Declaration of interests

The authors declare that they have no known competing financial interests or personal relationships that could have appeared to influence the work reported in this paper.

Funding statement

Authors declare that there is no funding was received to support this research work

Author information

Corresponding Author: Mohamed E. Mahmoud*

E-mail: memahmoud10@yahoo.com

Data availability

Data will be made available on request.

References

[1] Nie, Z., Luo, J., Tang, J., Li, B., Chen, B., Gao, M., ... & Guo, L. (2025). Pollution sources, characteristics and environmental risk assessment of heavy metals in surface water and sediments of typical pyrite mine in Southwest China. Journal of Environmental Sciences, 157, 742-755. https://doi.org/10.1016/j.jes.2025.01.008

[2] Li, Y., Zhang, J., Song, N., Wang, Y., Yu, J., He, L., ... & He, D. (2025). Assessment of health risk and identification of pollution sources of heavy metals in water in Chongqing's wastewater treatment plants based on ICP-MS. Environmental Pollution, 373, 126193. https://doi.org/10.1016/j.envpol.2025.126193

- [3] Wang, Z., Luo, P., Zha, X., Xu, C., Kang, S., Zhou, M., ... & Wang, Y. (2022). Overview assessment of risk evaluation and treatment technologies for heavy metal pollution of water and soil. Journal of Cleaner Production, 379, 134043. https://doi.org/10.1016/j.jclepro.2022.134043
- [4] Preonty, N., Hassan, M. N., Reza, A. H. M. S., Rasel, M. I. A., Mahim, M. M. A., & Jannat, M. F. (2025). Pollution and health risk assessment of heavy metals in surface water of the industrial region in Gazipur, Bangladesh. Environmental Chemistry and Ecotoxicology, 7, 527-538. https://doi.org/10.1016/j.enceco.2025.02.014
- [5] Meng, K., Dong, Y., Liu, J., Xie, J., Jin, Q., Lu, Y., & Lin, H. (2025). Advances in selective heavy metal removal from water using biochar: A comprehensive review of mechanisms and modifications, Journal of

- Environmental Chemical Engineering, 13, 116099. https://doi.org/10.1016/j.jece.2025.116099
- [6] Aziz, K. H. H., Mustafa, F. S., Omer, K. M., Hama, S., Hamarawf, R. F., & Rahman, K. O. (2023). Heavy metal pollution in the aquatic environment: efficient and low-cost removal approaches to eliminate their toxicity: a review. RSC advances, 13(26), 17595-17610. https://doi.org/10.1039/d3ra00723e
- [7] Luo, J. Z., Cai, Y. Y., Yu, J., Huang, J. F., & Yan, J. (2025). Phosphate-modified biochar-mineral-based composites for heavy metal removal in acidic environments: Development and efficiency. Applied Clay Science, *276*, 107924. https://doi.org/10.1016/j.clay.2025.107924
- [8] Althobaiti, S. A., Nabil, G. M., & Mahmoud, M. E. (2025). Insight into optimization of doxorubicin removal by a novel nanobiocomposite of doped molybdenum carbide and zinc ferrite onto pomegranate peels nanobiochar (Mo₂C-ZnFe₂O₄ PPNB). Journal of Molecular Liquids, 127597. https://doi.org/10.1016/j.molliq.2025.127597
- [9] Fekry, N. A., Mahmoud, M. E., Kamel, N. K., & Amira, M. F. (2025). Machine learning techniques for predicting the adsorption capacity of synergistic biochar functionalization with pyrrole-sulfanilic acid copolymer in mercury and chromium remediation. Chemical Engineering Journal, 503, 158322. https://doi.org/10.1016/j.cej.2024.158322
- [10] Mahmoud, S. E. M., Abdel-Fattah, T. M., Mahmoud, M. E., & Díaz, E. (2024). Facile doping and functionalization of molybdic acid into nanobiochar to enhance mercury ion removal from water systems. Nanomaterials, 14(22), 1789. https://doi.org/10.3390/nano14221789
- [11] Ervine, M., & Mangwandi, C. (2025). Evaluation of magnetic teawaste-based biochar particles for removal of cadmium from aqueous solutions. Particuology, 99, 92-105. https://doi.org/10.1016/j.partic.2025.02.007
- [12] Mukhrish, Y. E., & Amri, N. (2025). Environmental application of Typha Latifolia biochar/xanthan gum nanocomposite improved with thiosemicarbazide for the removal of cadmium ions from aqueous medium. International Journal of Biological Macromolecules, 145230. https://doi.org/10.1016/j.ijbiomac.2025.145230
- [13] Mei, Y., Gao, P., Li, J., He, X., Cui, L., Zhang, T., Wang, Y., & Xue, P. (2025). Enhanced cadmium sequestration from animal waste using a combined modified

- corn straw biochar: Unraveling the mechanisms and performance in hazardous metal removal. Environmental Technology & Innovation, 104256. https://doi.org/10.1016/j.eti.2025.104256
- [14] Wu, M., Wu, L., Zhang, W., Zhong, X., Guo, R., Cui, Z., Yang, Y., & Lv, J. (2025). Efficient removal of cadmium (II) and arsenic (III) from water by nanozero-valent iron modified biochar-zeolite composite. Ecotoxicology and Environmental Safety, 296, 118178. https://doi.org/10.1016/j.ecoenv.2025.118178
- [15] Li, S., Huang, Y., & Zhou, W. (2025). Simultaneous removal of cadmium and tetracycline from aqueous solutions by oxalic acid and pyrite co-modified biochar: Performance and mechanism. Environmental Research, 277, 121606. https://doi.org/10.1016/j.envres.2025.121606
- [16] Zhou, L. (2024). Improving the removal performance of cadmium from wastewater by phosphate-modified sludge biochar: A mineral dissolution-precipitation perspective, Desalination and Water Treatment, 320, 100865. https://doi.org/10.1016/j.dwt.2024.100865
- [17] Shah, A., Zakharova, J., Batool, M., Coley, M. P., Arjunan, A., Hawkins, A. J., ... & Williams, C. (2024). Removal of cadmium and zinc from water using sewage sludge-derived biochar. Sustainable Chemistry for the Environment, 6, 100118. https://doi.org/10.1016/j.scenv.2024.100118
- [18] Zhou, Z., Huang, L., Wang, H., & Chen, Y. (2024). Efficient removal of cadmium and lead in water by using nanomanganese oxide-loaded hydrochloric acid pretreated biochar. Journal of Environmental Chemical Engineering, 12(5), 113548. https://doi.org/10.1016/j.jece.2024.113548
- [19] Wang, X., Li, J., Xu, L., Su, J., Wang, Z., & Li, X. (2024). Simultaneous removal of calcium, cadmium and tetracycline from reverse osmosis wastewater by sycamore deciduous biochar, shell powder and polyurethane sponge combined with biofilm reactor. Bioresource Technology, 394, 130215. https://doi.org/10.1016/j.biortech.2023.130215
- [20] Bai, M., Chai, Y., Chen, A., Yuan, J., Shang, C., Peng, L., & Peng, C. (2024). Enhancing cadmium removal efficiency through spinel ferrites modified biochar derived from agricultural waste straw. Journal of Environmental Chemical Engineering, 11(1), 109027. https://doi.org/10.1016/j.jece.2022.109027

- [21] Song, Y., Tan, J., Jin, M., Liu, Z., Zhu, J., El-sayed, M. E., ... & Shen, Z. (2025). Effect of pyrolysis temperature and heating rate on the physicochemical properties of alkali lignin-derived biochar: A comparative study of fast and slow pyrolysis. Journal of Analytical and Applied Pyrolysis, 107236. https://doi.org/10.1016/j.jaap.2025.107236
- [22] Białowiec, A., & Syguła, E. (2026). Carbon-relative molar mass for the modeling of the lignocellulosic biomass torrefaction and slow pyrolysis performance and biochar fuel properties. Fuel, 403, 136119. https://doi.org/10.1016/j.fuel.2025.136119
- [23] Mahmoud, S. E. L. M. E., Ursueguia, D., Mahmoud, M. E., Abdel-Fattah, T. M., & Díaz, E. (2024). Functional surface homogenization of nanobiochar with cation exchanger for improved removal performance of methylene blue and lead pollutants. Biomass Conversion and Biorefinery, 14(16), 19107-19127. https://doi.org/10.1007/s13399-023-04098-9
- [24] Chai, W. S., Aslam, A. A., Li, X., Wu, T., & Pang, C. H. (2025). Surface-engineered biochar: Recent advances in modification strategies for environmental remediation and energy applications. Journal of Environmental Chemical Engineering, 13(5),117951. https://doi.org/10.1016/j.jece.202
 5.117951
- [25] Xu, T., Du, M., Yan, Y., & Singh, S. (2025). Wood-derived biochar for sustainable water remediation: insights into modification techniques, adsorption performance, techno-economic aspects, and future outlook. Journal of Molecular Structure, 1346, 143141. https://doi.org/10.1016/j.molstruc.2025.143141
- [26] Zhu, Y., Liu, S., Chen, H., Yu, P., & Chen, C. (2025). Evaluating biochar for adsorption of ammonium nitrogen in wastewater: insights into modifications and mechanisms. Environmental Research, 277, 121615. https://doi.org/10.1016/j.envres.2025.121615
- [27] Zhang, Y., Zhang, X., Zhou, Z., Liu, G., & Wang, C. (2025). A review of the conversion of wood biomass into high-performance bulk biochar: Pretreatment, modification, characterization, and wastewater application. Separation and Purification Technology, 361, 131448. https://doi.org/10.1016/j.seppur.2025.131448
- [28] Guo, W., Yao, X., Chen, Z., Liu, T., Wang, W., Zhang, S., ... & Wang, Y. (2024). Recent advance on application of biochar in remediation of heavy metal contaminated soil:

Emphasis on reaction factor, immobilization mechanism and functional modification. Journal of Environmental Management, 371, 123212.

https://doi.org/10.1016/j.jenvman.2024.123212

- [29] Animali, L., Corrado, S., Mitillo, N., Tuccimei, P., Bartoli, M., Mattei, M., & Giorcelli, M. (2025). Characterization and evaluation of commercial biochar for surface water purification. Sustainable Horizons, 15, 100145. https://doi.org/10.1016/j.horiz.2025.100145
- [30] Nguyen, D. T., Hoang, T. K., Tran, T. D., Nguyen, M. H., Trinh, K. T., Khuong, D. A., ... & Pham, T. D. (2025). Adsorption characteristics of individual and binary mixture of ciprofloxacin antibiotic and lead (II) on synthesized bamboobiochar. Environmental Research, 273, 121225. https://doi.org/10.1016/j.envres.2025.121225
- [31] Suratman, A., Astuti, D. N., Kusumastuti, P. P., Sudiono, S., Wijaya, H. W., & Wibowo, A. H. (2024). Comprehensive study of thermochemical conversion of biomass okara into biochar. Journal of Analytical and Applied Pyrolysis, 181, 106594. https://doi.org/10.1016/j.jaap.2024.106594
- [32] Panizio, R., Castro, C., Pacheco, N., Assis, A. C., Longo, A., Vilarinho, C., ... & Nobre, C. (2024). Investigation of biochars derived from waste lignocellulosic biomass and insulation electric cables: A comprehensive TGA and Macro-TGA analysis. Heliyon, 10(18), e37882. https://doi.org/10.1016/j.heliyon.2024.e37882
- [33] Baath, Y. S., Nikrityuk, P. A., & Gupta, R. (2022). Experimental and numerical verifications of biochar gasification kinetics using TGA. Renewable Energy, 185, 717-733. https://doi.org/10.1016/j.renene.2021.12.091
- [34] Mahmoud, M. E., Nabil, G. M., Althobaiti, S. A., & Elsayed, S. M. (2024). Effective solid–solid and microwave-assisted formation of folic acid@ titanium oxide nanoparticles for enhanced batch adsorptive uptake of toxic Cd (II) and Cu (II) pollutants. Inorganic Chemistry Communications, 162, 112242. https://doi.org/10.1016/j.inoche.2024.112242
- [35] Sidabutar, R., Trisakti, B., Gusty, N. D., Syahputra, M. R., Saputra, B. W., Alexander, V., ... & Abdul, P. M. (2024). Towards low-cost and sustainable biochar production based on empty fruit bunch: Effect of pelletization, microwave power, residence time, and mass on biochar quality for commercial approach. Case Studies in Chemical and Environmental

Engineering, 10,100929. https://doi.org/10.1016/j.cscee.2024. 100929

[36] Barkhordari, M. S., & Qi, C. (2025). Integrating machine learning and reliability analysis: A novel approach to predicting heavy metal removal efficiency using biochar. Ecotoxicology and Environmental Safety, 299, 118381. https://doi.org/10.1016/j.ecoenv.2025.118381

[37] Ye, M., Li, Z., Wen, L., Duan, F., & Zhang, L. (2025). Enhanced Cr (VI) removal via surfactant-tailored magnetic functionalized-biochar: Synergistic alkyl grafting and iron dispersion for broad-spectrum pH adaptability. Journal of Environmental Chemical Engineering, 13(5), 117877. https://doi.org/10.1016/j.jece.2025.117877

[38] Li, Z., Zhou, Y., Yin, Q., & Ma, L. (2024). Simultaneous removal of lead (II) and cadmium (II) from acidic wastewater by Fe-modified sludge biochar. Desalination and Water Treatment, 320,

https://doi.org/10.1016/j.dwt.2024.100716

[39] Tuyiringire, D., Liu, X., Zheng, Q., Wang, S., Zhang, W., Bi, F., ... & Zhang, Y. (2025). Ball-milled phosphate/micro zero-valent iron/biochar for lead and cadmium removal and stabilization in water and soil: Performance, mechanisms, and environmental applications. Separation and Purification Technology, 362,131895. https://doi.org/10.1016/j.seppur.202 5.131895

[40] Wang, Y., Li, J., Li, Q., Xu, L., Ai, Y., Liu, W., ... & Zhang, Y. (2024). Effective amendment of cadmium in water and soil before and after aging of nitrogen-doped biochar: Preparation optimization, removal efficiency and mechanism. Journal of Hazardous Materials, 477, 135356. https://doi.org/10.1016/j.jhazmat.2024.135356

[41] Zhou, Q., Huang, Y., Liu, L., Li, Z., Xiao, Y., Li, Z., ... & Pan, H. (2025). Enhanced cadmium adsorption by silicate-modified biochar derived from sawdust: Mechanisms and performance analysis. Surfaces and Interfaces, 65, 106430. https://doi.org/10.1016/j.surfin.2025.106430

[42] Foroutan, R., Peighambardoust, S. J., Ghojavand, S., Farjadfard, S., & Ramavandi, B. (2023). Cadmium elimination from wastewater using potato peel biochar modified by ZIF-8 and magnetic nanoparticles. Colloid and Interface Science Communications, 55, 100723. https://doi.org/10.1016/j.colcom.2023.100723

[43] Park, C. M., Han, J., Chu, K. H., Al-Hamadani, Y. A., Her, N., Heo, J., & Yoon, Y. (2017). Influence of solution pH, ionic strength, and humic acid on cadmium adsorption onto activated biochar: Experiment and modeling. Journal of Industrial and Engineering Chemistry, 48, 186-193. https://doi.org/10.1016/j.jiec.2016.12.038

[44] Nabil, G. M., & Mahmoud, M. E. (2024). Superior adsorptive uptake of methylene blue pollutant by nanobiochar-impregnated-layered double hydroxides. Inorganic Chemistry Communications, 168, 112913. https://doi.org/10.1016/j.inoche.2024.112913